IEEE Access
Multidisciplinary | Rapid Review | Open Access Journal

Received August 8, 2020, accepted August 19, 2020, date of publication August 24, 2020, date of current version September 8, 2020.

Digital Object Identifier 10.1109/ACCESS.2020.3019026

Cooperative Spectrum Sensing Using Maximum a Posteriori as a Detection Technique for Dynamic Spectrum Access Networks

AHMED TOHAMY[1], USAMA SAYED MOHAMED[1], MOHAMMAD M. ABDELLATIF[2], (Senior Member, IEEE), TAHA A. KHALAF[1], (Member, IEEE), AND MOHAMED ABDELRAHEEM[1], (Member, IEEE)

[1]Electrical Engineering Department, Faculty of Engineering, Assiut University, Assiut 71515, Egypt
[2]Electrical Engineering Department, Faculty of Engineering, The British University in Egypt, El Sherouk City, Cairo 11837, Egypt

Corresponding author: Ahmed Tohamy (tohamymt@aun.edu.eg)

ABSTRACT Over the past few years, dynamic spectrum access has been gaining an increasing attention as a solution to the spectrum scarcity problem. In this paper, a primary user detection technique based on Maximum A Posteriori estimation is proposed for dynamic spectrum access networks. In the proposed technique, a set of secondary users acting as sensing nodes send their individual decisions about the existence of the primary user to a central fusion center. The fusion center uses the received data to form a codeword then, applies the maximum a posteriori estimation rule to make a final decision regarding the presence of the primary user. The proposed technique takes into consideration the accuracy of the local decisions provided by the secondary users when making a final decision. In this paper, we analyze the performance of the proposed scheme and derive closed-form expressions for the upper bounds of the false alarm and misdetection probabilities. The results show that the proposed technique outperforms other combining techniques in terms of its ability to detect the primary user and, accordingly, minimizes the harmful interference to the licensed network. Moreover, the proposed technique achieves better performance at a lower number of reporting secondary users which compensates for the complexity of the maximum a posteriori estimation.

INDEX TERMS Cognitive radio, cooperative sensing, spectrum sensing, fusion center, maximum a posteriori.

I. INTRODUCTION

The rapid development in wireless technologies created a large demand on the frequency spectrum, which is not satisfied using the current spectrum management policies [1]. However, studies show that the problem is mainly due to the inefficient utilization of the available spectrum rather than the scarcity of free spectrum bands. For example, in a study on the spectrum utilization in the United States, results showed that around 75% of the reserved spectrum bands are free and not utilized by their incumbent users [2]. Dynamic Spectrum Access (DSA) has been proposed as a solution for the inefficient utilization of the frequency spectrum problem [3]. In DSA systems, unlicensed users (known as Secondary Users (SUs)) are allowed to access and utilize the frequency bands/time slots of the incumbent users (known as the Primary Users (PUs)) for a certain period, and only at a given location such that they do not cause service degradation for the PUs [4]. The realization of practical DSA systems is not possible with SUs equipped with conventional transceivers as additional functions have to be performed by the SUs in DSA systems. Cognitive Radio (CR) is the enabling technology behind DSA systems. An SU equipped with CR technologies gains some intelligence as it becomes able to perform additional tasks like spectrum sensing, modulation technique recognition, and adaptive transmission [5]. As the main goal of DSA is to utilize the unused spectrum without causing a harmful interference to the PUs, the ability of SUs to detect the PUs is a crucial function that must be performed by the secondary system. Spectrum Sensing (SS) is the name of the CR process responsible for detecting the presence of the PU in DSA systems, and it is also considered the first step of the cognitive radio cycle [6], [7].

To quantify and evaluate any detection mechanism, false alarm (FA) and misdetection (MD) probabilities must be calculated. The FA probability indicates how frequently the

The associate editor coordinating the review of this manuscript and approving it for publication was Ding Xu.

detector wrongly declares that the PU is active utilizing its frequency band. This wrong decision causes the SU to miss the opportunity to utilize the PU's free frequency band. On the other hand, the MD probability indicates how frequently the detector decides that the PU is absent while it is not. This wrong decision may cause transmission collision or harmful interference if the SU transmitted its signal on the occupied band [8].

The presence of the PU is checked by detecting its signal over the targeted frequency band using different methods. These methods are mainly categorized into two approaches. The first one is a blind sensing technique, in which the SUs don't need any pre-known information about the transmitted signal like in the Energy Detection (ED) technique. The ED is widely used for SS function because of its implementation simplicity, and the low design complexity [9], [10]. In the ED technique, the SU needs to estimate only the noise power to set the threshold value and does not require any information about the PU transmission characteristics such as modulation technique or data rate [11], [12].

The other approach is the signal-specific sensing technique, in which the SUs need some knowledge about the characteristics of the PU's signal such as symbol period, modulation type, and carrier frequency, etc. [13]. The most used methods for spectrum sensing in this approach are matched filter detection, and cyclostationary feature detection [14].

The other way to categorize the SS function is based on the level of cooperation between the secondary network members. In this classification, the SS function is carried out either individually or cooperatively. In individual SS, each SU performs the necessary task to detect the PU individually and takes a decision based on its own capability and geographical location without any help from other SUs and without sharing its sensing information with others. On the other hand, SUs may cooperate by sharing their sensing information to achieve a more accurate PU detection result and hence it's named cooperative spectrum sensing. Cooperative spectrum sensing is able to mitigate hidden-node problems [15], and to increase the reliability of detecting PU's activities at low PU signal-to-noise ratios (SNRs) [16].

In cooperative sensing, the final decision about the presence of the PU is taken either by individual SUs in a distributed fashion or by a centralized entity. In distributed sensing, each SU is responsible for taking an individual decision after collecting sensing information from all other neighboring SUs. In centralized sensing, the decision is made at a central entity called the Fusion Center (FC) after collecting individual SU's sensing information. In both categories, the shared sensing information can be in one of three forms: raw-sensing data (samples of the received signal), processed data, or individual decisions. Generally, the sensing results received by the FC or shared with other SUs are combined to perform the cooperative sensing and to obtain the final decision about the PU presence [15].

The most popular combining techniques used in centralized cooperative sensing are Equal Gain Combining (EGC) [17], Maximal Ratio Combining (MRC) [18], and Selection Combining (SC) [19] as will be presented in section II.

In this paper, we propose a centralized cooperative spectrum sensing framework that is based on Maximum A Posteriori (MAP) detection for DSA networks. In this framework, the sensing process occurs in two successive phases. In the first phase, the SUs use the energy detection technique to make local (individual) decisions then, forward the sensing information to the FC. In the second phase, the FC uses the received data to form a codeword then, applies the MAP detection technique to make the final decision about the presence of the PU. The MAP detector determines the most probable hypothesis given the data. Since no other hypothesis is more likely, the decision provided is the optimal one. Moreover, as will be presented in Section IV, the MAP detection takes into consideration the reliability of local sensing information received from the SUs. The reliability of decisions is measured and incorporated into the MAP detection rule using local false alarm and misdetection probabilities (i.e., false alarm and misdetection done by SUs individually). This can be considered as if the FC assigns weights in an optimal manner to individual decisions in order to make the final decision. Therefore, the proposed scheme is expected to outperform other combining techniques used at the FC.

Our contribution in this paper can be summarized as follows:

- Proposing a MAP-based centralized cooperative spectrum sensing technique for DSA networks. The proposed scheme is optimal in the sense of minimizing the false alarm and misdetection probabilities at the FC.
- Analyzing the performance of the proposed scheme by deriving a mathematical closed-form expression for the upper bounds of the false alarm and misdetection probabilities.

Additionally, we compare the performance of the proposed detection mechanism with other techniques found in the literature and with the theoretical upper bounds.

Organization of paper is as follows: The related work is presented in Section II. The system model is described in Section III. The MAP-based detection technique is described in Section IV. Section V presents the derivation of the upper bounds for the proposed system. Section VI presents the performance evaluation of the proposed technique. Finally, the conclusions are drawn in Section VII.

II. RELATED WORK

In this section, we discuss recent related work in cooperative spectrum sensing for DSA systems. In cooperative sensing, combining individual decisions from SUs can be performed in two different ways according to the available bandwidth for the control channel [4], [15]:

- Soft combining: The SUs send the whole sensing samples or the complete sensing results to the FC. Existing receiver diversity techniques such as SC, EGC, and MRC can be utilized for soft combining of local observations or test statistics.
- Hard combining: The SUs transmit the one-bit decisions to the FC. The commonly used fusion rules are AND, OR, and majority voting rules. The OR rule works better when the number of cooperating SUs is large. Similarly, the AND rule works better when the number of reporting SUs users is small [20].

The main benefit of soft combining is its higher accuracy result compared to hard combining which consumes less bandwidth in reporting the SUs detection results. In MRC combining technique, the signals from each SU are co-phased and weighted before being combined. The applied weights have to be adjusted according to the estimated channels between the SUs and the FC [17]. The EGC technique is similar to MRC except for the weighting circuits [18]. A performance comparison between the MRC and EGC as combining techniques for cooperative spectrum sensing in cognitive radio networks is provided in [21]. In the SC approach, the output performance of the combining process is the same as the highest SNR among all received signals. Using the soft combining technique for making a decision using the one-bit individual decision from each SU is also used. A quantized equal gain combining (QEGC) technique, presented in [22], gives a good balance between the two benefits. Moreover, in [23], authors show how the MRC technique can be used to get a better performance than the majority voting technique when used at the FC. Furthermore, Hybrid techniques are usually used to achieve a trade-off between the benefits of the good performance of the soft combining and the low communication cost of the hard combining. An example of such a hybrid system is presented in [24] where a clustered distributed detection system using a fuzzy logic system and a fuzzy c-means clustering algorithm is developed.

The authors of [25] proposed a cooperative blind Bayesian-based detection framework for spectrum sensing in CR networks to overcome the noise variance uncertainty problem which severely degrades the performance of the ED. In [25], M SUs calculate the power of observed signals and forward it to the FC. Then, the FC utilizes the proposed algorithm to blindly make the final decision about the existence of the primary user. The proposed algorithm is designed mainly for low SNR scenario (e.g., -22dB) and, accordingly, it requires a large window size for power calculations (at least 1000 time instants). Although the proposed framework provides a good performance in terms of false alarm and misdetection probabilities, the authors assume error-free links between the SUs and the FC.

MAP rule was used in SUs to enhance the ability of detection by solving the uncertain noise energy problem that appears when the energy detection technique is used. In this technique, the spectrum sensing is performed in two steps. First, the posterior probability of each state is estimated using the structure of the Bayesian network, then the posterior probability can be used as the prior probability for the MAP approach [26].

The MAP estimator has been used at the FC by Zhou *et.al.* [27]. Progressive MAP algorithm was used at the FC as a binary energy detection technique to recover the transmitted decisions stream received from the SUs, which can be considered as passing a two-state Markov chain. However, the final decision is made using hard combining techniques (majority voting/OR techniques).

As a combining technique, authors of [28] developed a MAP-based technique in the relay-based network to improve the recovery of the originally transmitted signal. The detector constructs a codeword from both the relayed and the directly transmitted signals. It uses MAP to estimate the originally transmitted data.

In our proposed system, the MAP algorithm is used alone at the FC and independent of any other decision techniques. This is different from the other mentioned systems that use MAP at the SUs or the FC to enhance the detection of the received bits and use other combining techniques to obtain the final decision.

TABLE 1. The list of symbols.

Symbol	Description
M	The number of SUs
y_{SU_n}	The received signal at the n-th SU
y_{FC_n}	The received signal from the n-th SU
h_{SU_n}	The Rayleigh flat fading channel gains (PU$\rightarrow$ SU)
h_{FC_n}	The Rayleigh flat fading channel gains (SU$\rightarrow$ FC)
x_{PU}	The BPSK modulated signal as the PU transmitted bit
x_{SU_n}	The BPSK modulated signal corresponding to the n-th SU
CW_i	The transmit codeword from SUs
X_i	The transmit vector corresponding to the codeword CW_i
w_{SU_n}	The AWGN with zero mean and variances $N_{0SU_n}/2$
w_{FC_n}	The AWGN with zero mean and variances $N_{0FC_n}/2$
P_D	The probability of detection
P_{MD}	The probability of misdetection
P_{FA}	The probability of false alarm
TH	The selected detection threshold used in ED receiver
$\sigma^2_{w_n}$	The noise variance at n-th SU
γ_{SU_n}	The receive SNR at n-th SU
Γ	The channel goodness indicator $= \sqrt{\gamma_{FC}/(1+\gamma_{FC})}$
$\Gamma(.)$	The Gamma function
$\Gamma(.,.)$	The incomplete Gamma function
ϑ_{ki}	The ratio between $P(CW_k)$ and $P(CW_i)$
δ_{ki}	The hamming distance between $P(CW_k)$ and $P(CW_i)$
l_h	The number of bits that can represent the channel coeff. h
l_s	The number of bits that can represent Y from the SU
l_p	The number of bits that can represent $P(CW_i)$

III. SYSTEM MODEL

The system and network models are shown in Fig. 1, and the symbols used in this paper are listed in Table 1. In the secondary network, we have the FC and M SUs acting as sensing nodes which cooperate to detect the PU status. The detection of the PU signal is performed in two phases. In the first one, each SU makes a local decision about the existence

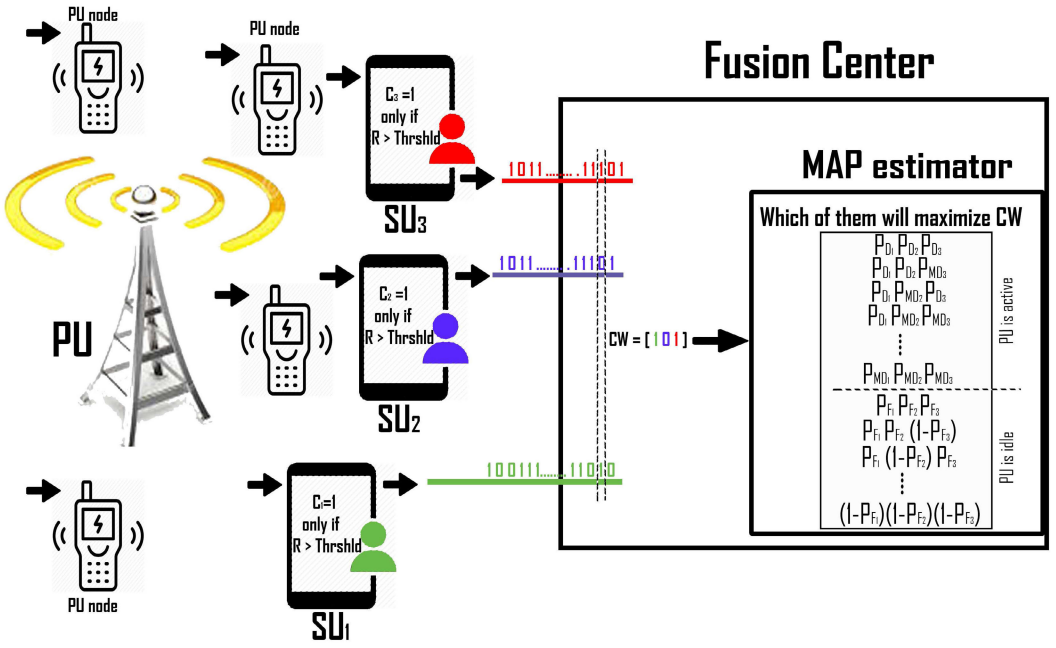

FIGURE 1. System model for centralized cooperative CR network.

of the PU signal individually and forwards the sensing results to the FC. The SU detects the existence of the PU using ED technique where the energy of the received signal is calculated and compared to a pre-defined threshold TH. The SU transmits $+1$ symbol if the PU is detected (i.e., the energy of the received signal is greater than or equal to TH) and -1 if not.

In the second phase, the FC constructs a codeword from the data received from all SUs and applies the MAP-based detector to make a final decision about the presence of the PU. In this paper, we assume that the PU and all the SUs transmit their data using Binary Phase Shift Keying (BPSK) modulation and that the channels between network nodes experience Rayleigh flat fading with Additive White Gaussian Noise (AWGN). The signal received from the PU at the n-th SU is given by

$$y_{SU_n} = h_{SU_n} x_{PU} + w_{SU_n}, \tag{1}$$

and the signal received from the n-th SU at the FC is given by

$$y_{FC_n} = h_{FC_n} x_{SU_n} + w_{FC_n}, \tag{2}$$

where:

- $x_{PU} \in \{-\sqrt{E_s}, 0, +\sqrt{E_s}\}$ is the BPSK modulated signal corresponding to the PU's transmitted bit $C_s \in \{-1, 0, +1\}$ with $P(C_s) \in \{0.25, 0.5, 0.25\}$, respectively, where E_s is the energy of the PU bit.
- $x_{SU_n} \in \{-\sqrt{E_{SU_n}}, +\sqrt{E_{SU_n}}\}$ is the BPSK modulated signal corresponding to the n-th SU decision bit $C_{SU_n} \in \{-1, +1\}$ where E_{SU_n} is the energy of the n-th SU bit.
- $h_{SU_n}$and h_{FC_n} are Rayleigh flat fading channel gains of the links between the PU and the n-th SU and between the n-th SU and the FC, respectively, where $E[h^2_{SU_n}] = E[h^2_{FC_n}] = 1$.
- w_{SU_n} and w_{FC_n} are AWGN with zero mean and variances $N_{0SU_n}/2$, and $N_{0FC_n}/2$ at the SU receiver and at the FC receiver, respectively.

The signals received at the FC from M SUs can be written in a matrix form as follows

$$\boldsymbol{Y} = \boldsymbol{H}\boldsymbol{X} + \boldsymbol{W} \tag{3}$$

where $\boldsymbol{Y} = [y_{FC_1} y_{FC_2} \ldots . y_{FC_M}]^T$, $\boldsymbol{X} = [x_{SU_1} x_{SU_2} \ldots . x_{SU_M}]^T$, $\boldsymbol{W} = [w_{FC_1} w_{FC_2} \ldots . w_{FC_M}]^T$, and the channel matrix $\boldsymbol{H}$ is given by

$$\boldsymbol{H} = \begin{bmatrix} h_{FC_1} & 0 & 0 & \ldots\ldots & 0 \\ 0 & h_{FC_2} & 0 & \ldots\ldots & 0 \\ . & \ldots\ldots & \ldots\ldots & & \\ . & & & & \\ . & & & & \\ 0 & 0 & 0 & \ldots\ldots & h_{FC_M} \end{bmatrix}. \tag{4}$$

The received vector $\boldsymbol{Y}$ is used by the MAP-based detector to make the final decision about the PU status. This decision depends on the quality of the channels between the PU and the SUs, the detection thresholds used by the SUs, and the quality of the channels between the SUs and the FC.

IV. MAP-BASED DETECTION TECHNIQUE

Unlike the majority voting and MRC techniques, the MAP-based detection technique takes into consideration the quality of the detection links between the PU and the SUs. The quality of these links is measured using false alarm and misdetection probabilities. These probabilities are passed to the MAP detection algorithm together with the received vector $\boldsymbol{Y}$ to make the final decision about the existence of the PU. The MAP detection technique is optimal in the sense that it minimizes the false alarm and misdetection probabilities at the FC [29].

TABLE 2. MAP decision scheme for a case of three SUs.

PU Status	codeword		P(CW_i)
Active	CW_1	+1 +1 +1	$P_{D_1}P_{D_2}P_{D_3}$
	CW_2	+1 +1 -1	$P_{D_1}P_{D_2}P_{MD_3}$
	CW_3	+1 -1 +1	$P_{D_1}P_{MD_2}P_{D_3}$
	CW_4	+1 -1 -1	$P_{D_1}P_{MD_2}P_{MD_3}$
	CW_5	-1 +1 +1	$P_{MD_1}P_{D_2}P_{D_3}$
	CW_6	-1 +1 -1	$P_{MD_1}P_{D_2}P_{MD_3}$
	CW_7	-1 -1 +1	$P_{MD_1}P_{MD_2}P_{D_3}$
	CW_8	-1 -1 -1	$P_{MD_1}P_{MD_2}P_{MD_3}$
Idle	CW_9	+1 +1 +1	$P_{FA_1}P_{FA_2}P_{FA_3}$
	CW_{10}	+1 +1 -1	$P_{FA_1}P_{FA_2}(1-P_{FA_3})$
	CW_{11}	+1 -1 +1	$P_{FA_1}(1-P_{FA_2})P_{FA_3}$
	CW_{12}	+1 -1 -1	$P_{FA_1}(1-P_{FA_2})(1-P_{FA_3})$
	CW_{13}	-1 +1 +1	$(1-P_{FA_1})P_{FA_2}P_{FA_3}$
	CW_{14}	-1 +1 -1	$(1-P_{FA_1})P_{FA_2}(1-P_{FA_3})$
	CW_{15}	-1 -1 +1	$(1-P_{FA_1})(1-P_{FA_2})P_{FA_3}$
	CW_{16}	-1 -1 -1	$(1-P_{FA_1})(1-P_{FA_2})(1-P_{FA_3})$

To describe the proposed algorithm, we consider a secondary network composed of three SUs and one FC. However, the same procedure can be generalized to support an arbitrary number of SUs. Let $CW = \left[C_{SU_1}\ C_{SU_2}\ C_{SU_3}\right]^T$ be the codeword of the individual detection decisions sent by the SUs to the FC. If the channels between the PU and the SUs have the same quality (i.e equal received SNRs), and all of the SUs use the same detection threshold TH, this codeword will take one of two values $[+1\ +1\ +1]^T$ or $[-1\ -1\ -1]^T$. Since, in general, these channels don't necessarily have the same quality, this codeword will take one of eight possible values. The probability of sending a codeword depends on the status of the PU (active or idle) as illustrated in Table 2 where P_{D_n}, P_{MD_n}, and P_{FA_n} are the local probabilities of detection, misdetection, and false alarm, respectively, at the n^{th} SU. The values of these local probabilities are calculated according to the following equations [30]–[32]

$$P_{MD_n} = 1 - \Gamma\left(1, \frac{\sqrt{TH}}{\sqrt{\sigma^2_{w_n}}\left(1+\sqrt{\gamma_{SU_n}}\right)}\right) \tag{5}$$

$$P_{D_n} = 1 - P_{MD_n} \tag{6}$$

$$P_{FA_n} = 2Q\left(\sqrt{\frac{TH}{\sigma^2_{w_n}}}\right) \tag{7}$$

where $\sigma^2_{w_n} = N_{0SU_n}/2$ is the noise variance at n-th SU, $\gamma_{SU_n} = E_s/N_{0SU_n}$ is the received SNR at n-th SU, and $\Gamma(.,.)$ is the incomplete Gamma function. For mathematical traceability, we assign two different indices to the same codeword in order to represent the difference in its probability (i.e., $CW_{i+8} = CW_i$ but $P(CW_{i+8}) \neq P(CW_i)$).

The MAP detection technique estimates the transmitted codeword $\widehat{CW}$ as follow:

$$\begin{aligned}\widehat{CW} &= \arg\max_{CW_i} P(CW_i|Y) \\ &= \arg\max_{CW_i} \frac{P(Y|CW_i)P(CW_i)}{P(Y)}. \\ &= \arg\max_{CW_i} P(Y|CW_i)P(CW_i)\end{aligned} \tag{8}$$

where the maximization process occurs over the sixteen possible codewords provided in Table 2,

$$P(Y|CW_i) = \frac{1}{(\pi N_{0FC})^{3/2}} e^{-\|Y-HX_i\|^2/N_{0FC}}, \tag{9}$$

and X_i is the transmitted vector corresponding to the codeword CW_i, e.g., $X_2 = \left[+\sqrt{E_{SU_1}} + \sqrt{E_{SU_2}} - \sqrt{E_{SU_3}}\right]^T$. Substituting from (9) into (8) yield

$$\begin{aligned}\widehat{CW} &= \arg\max_{CW_i}\left(\frac{P(CW_i)}{(\pi N_{0FC})^{3/2}} e^{-\|Y-HX_i\|^2/N_{0FC}}\right) \\ &= \arg\min_{CW_i}\left(\|Y-HX_i\|^2 - N_{0FC}\ log\left(P(CW_i)\right)\right)\end{aligned} \tag{10}$$

After estimating the codeword $\widehat{CW}$, the FC makes a decision about the PU status as follows

- PU is active if $\widehat{CW} \in \{CW_1, CW_2, \ldots . CW_M\}$
- PU is idle if $\widehat{CW} \in \{CW_{M+1}, CW_{M+2}, \ldots . CW_{2M}\}$

Algorithm 1 depicts the operation of proposed MAP-based detection technique at the FC.

Algorithm 1 The Proposed MAP-Based Technique as a Detection System at the FC

Input : Y, H, $P(CW_i)$, and N_{0FC}
Output: PU status
for ($i = 1$ ***to*** 2^M) **do** // All Possible CodeWords for M Secondary Users
  Calculate
  $K_{A_i} \leftarrow \|Y - HX_i\|^2 - N_{0FC}\ log\left(P(CW_i)\right)$
  $K_{I_i} \leftarrow \|Y - HX_i\|^2 - N_{0FC}\ log\left(P(CW_{i+2^M})\right)$
end
$K_{A_{min}} \leftarrow \min(K_{A_1} K_{A_2} \ldots K_{A_{2^M}})$
$K_{I_{min}} \leftarrow \min(K_{I_1} K_{I_2} \ldots K_{I_{2^M}})$
if $K_{A_{min}} < K_{I_{min}}$ **then**
  PU status $\leftarrow$ PU is Active
else
  PU status $\leftarrow$ PU is Idle
end
return PU status

V. SYSTEM PERFORMANCE

In this section, in order to analyze the performance of the proposed technique, we derive closed-form expressions for the upper bounds on the final false alarm and misdetection probabilities (i.e., P_{FA}, and P_{MD} at the FC). The derived expressions are used to determine the theoretical limits of the system performance and for the sake of comparison with other techniques.

For M SUs, the probabilities of false alarm and misdetection are given by

$$P_{FA} \leq \sum_{k=2^M+1}^{2^{M+1}} \sum_{i=1}^{2^M} P\left(CW_k \rightarrow CW_i\right) P\left(CW_k\right) \tag{11}$$

and

$$P_{MD} \leq \sum_{k=1}^{2^M} \sum_{i=2^M+1}^{2^{M+1}} P\left(CW_k \rightarrow CW_i\right) P\left(CW_k\right), \quad (12)$$

respectively, where $P\left(CW_k \rightarrow CW_i\right)$ is the pairwise error probability of confusing CW_k with CW_i when CW_k is transmitted and when these are the only two hypotheses.

$P(CW_k)$ can be calculated by substituting from (5), (6), and (7) into codewords probabilities given in Table 2. In order to calculate the upper bounds on P_{FA} and P_{MD} (i.e., the right hand sides of (11) and (12)), we need to derive an analytical expression for $P\left(CW_k \rightarrow CW_i\right)$ for all possible values of i, k. In the mathematical analysis, we continue with the assumption of having three SUs. However, following the same outlines, the derivation can be generalized to support an arbitrary number of SUs.

When the transmitted codeword is CW_k, the received vector would be $Y_k = HX_k + \boldsymbol{W}$. According to (10), the probability $P\left(CW_k \rightarrow CW_i\right)$ is given by (13), as shown at the bottom of the next page, where $\langle \boldsymbol{W}, H\left(X_k - X_i\right)\rangle$ denotes the dot product of the two vectors $\boldsymbol{W}$ and $H\left(X_k - X_i\right)$. When $\boldsymbol{h} = \left[h_{SU_1}\ h_{SU_2}\ h_{SU_3}\right]^T$ is given, $\langle \boldsymbol{W}, H\left(X_k - X_i\right)\rangle$ would be a zero mean Gaussian random variable with variance $\frac{N_0}{2}\left\|H\left(X_k - X_i\right)\right\|^2$. Accordingly,

$$P\left(CW_k \rightarrow CW_i | \boldsymbol{h}\right) = Q\left(\frac{\left\|H\left(X_k - X_i\right)\right\|}{\sqrt{2N_0}} + \frac{\sqrt{N_0/2}\, log\left(\vartheta_{ki}\right)}{\left\|H\left(X_k - X_i\right)\right\|}\right) \quad (14)$$

where $\vartheta_{ki} = P\left(CW_k\right)/P\left(CW_i\right)$. In order to find $P\left(CW_k \rightarrow CW_i\right)$, (14) has to be averaged over the distribution of the random variable $\left\|H\left(X_k - X_i\right)\right\|$. Since gains of all channels have the same distribution, then, the distribution of the $\left\|H\left(X_k - X_i\right)\right\|$ depends on the hamming distance between CW_k and CW_i, i.e., the number of positions at which CW_k and CW_i are different. In what follows, the hamming distance between CW_k and CW_i will be denoted by δ_{ki} where $\delta_{ki} \in \{0, 1, 2, 3\}$. Hence, the distribution of the $\left\|H\left(X_k - X_i\right)\right\|$ would be the same for any pair of codewords with the same δ_{ki}. Therefore, the probability $P\left(CW_k \rightarrow CW_i\right)$ depends on:

1) The hamming distance δ_{ki}
2) The ratio between codewords probabilities ϑ_{ki}.

Let $\rho_{\delta_{ki}}\left(\vartheta_{ki}\right) = P\left(CW_k \rightarrow CW_i\right)$. Then, we need to derive $\rho_{\delta_{ki}}\left(\vartheta_{ki}\right)$ for $\delta_{ki} \in \{0, 1, 2, 3\}$.

- Derivation of $\rho_0\left(\vartheta_{ki}\right)$
  Since $\rho_0\left(\vartheta_{ki}\right) = P\left(CW_k \rightarrow CW_i\right)$ when $CW_k = CW_i$ (but $P(CW_k) \neq P(CW_i)$), we can not use (14) to continue our derivation and we have to go one step backwards. From (13),

$$\begin{aligned}\rho_0 &= P\left(log\left(\frac{P(CW_k)}{P(CW_i)}\right) < 0\right) \\ &= P\left(log\left(\vartheta_{ki}\right) < 0\right)\end{aligned} \quad (15)$$

Since $P(CW_k)$ and $P(CW_i)$ are deterministic variables, then

$$\rho_0\left(\vartheta_{ki}\right) = \begin{cases} 0 & \vartheta_{ki} \geq 1 \\ 1 & \vartheta_{ki} < 1 \end{cases} \quad (16)$$

- To derive $\rho_1\left(\vartheta_{ki}\right)$, we consider the case when $k = 3$ and $i = 7$ that can be generalized to all values of k and i such that $\delta_{ki} = 1$. From (14),

$$\begin{aligned}&P\left(CW_3 \rightarrow CW_7 | \boldsymbol{h}\right) \\ &= Q\left(\frac{\left\|H\left(X_7 - X_3\right)\right\|}{\sqrt{2N_0}} + \frac{\sqrt{N_0/2}\, log\left(\vartheta_{73}\right)}{\left\|H\left(X_7 - X_3\right)\right\|}\right) \\ &= Q\left(\sqrt{2h_{SU_1}^2 \gamma_{FC}} + \frac{log\left(\vartheta_{73}\right)}{2\sqrt{2h_{SU_1}^2 \gamma_{FC}}}\right)\end{aligned} \quad (17)$$

Averaging (17) over distribution of $h_{SU_1}^2$, yields

$$\rho_1\left(\vartheta_{ki}\right) = \begin{cases} \frac{1-\Gamma}{2}\, \vartheta_{ki}^{-\left(1+\frac{1}{\Gamma}\right)/2} & \vartheta_{ki} \geq 1 \\ 1 - \frac{1+\Gamma}{2}\, \vartheta_{ki}^{-\left(1-\frac{1}{\Gamma}\right)/2} & \vartheta_{ki} < 1 \end{cases} \quad (18)$$

where $\Gamma = \sqrt{\gamma_{FC}/(1+\gamma_{FC})}$, and the derivation of (18) is provided in Appendix VII.

- To derive $\rho_2\left(\vartheta_{ki}\right)$ considering the case when $k = 4$ and $i = 6$ (and which imply generally, $\{\forall\, i, k : \delta_{ki} = 2\}$)

$$\begin{aligned}\rho_2\left(\vartheta_{46}\right) &= P\left(CW_4 \rightarrow CW_6 | \boldsymbol{h}\right) \\ &= Q\left(\sqrt{2\left(h_{SU_1}^2 + h_{SU_2}^2\right)\gamma_{FC}} + \frac{log\left(\vartheta_{ki}\right)}{2\sqrt{2\left(h_{SU_1}^2 + h_{SU_2}^2\right)\gamma_{FC}}}\right) \\ &= Q\left(\sqrt{2Z_2} + \frac{log\left(\vartheta_{ki}\right)}{2\sqrt{2Z_2}}\right)\end{aligned} \quad (19)$$

where $Z_2 = \left(h_{SU_1}^2 + h_{SU_2}^2\right)\gamma_{FC}$. Since $h_{SU_1}^2$ and $h_{SU_2}^2$ have an exponential distribution, the distribution of their summation Z_2 is given by [33], [34].

$$f_z\left(Z_2\right) = \frac{1}{\gamma_{FC}^2} Z_2\, e^{-Z_2/\gamma_{FC}}, \quad (20)$$

Averaging (19) over the distribution of Z_2 which is given in (20) yields to (23), as shown at the bottom of the 8th page; the derivation is given in the Appendix VII.

- To derive $\rho_3\left(\vartheta_{ki}\right)$ considering the case when $k = 2$ and $i = 7$ (and which imply generally, $\{\forall\, i, k : \delta_{ki} = 3\}$)

$$\begin{aligned}\rho_3\left(\vartheta_{27}\right) &= P\left(CW_2 \rightarrow CW_7 | \boldsymbol{h}\right) \\ &= Q\left(\sqrt{2\left(h_{SU_1}^2 + h_{SU_2}^2 + h_{SU_3}^2\right)\gamma_{FC}} + \frac{log\left(\vartheta_{ki}\right)}{2\sqrt{2\left(h_{SU_1}^2 + h_{SU_2}^2 + h_{SU_3}^2\right)\gamma_{FC}}}\right) \\ &= Q\left(\sqrt{2Z_3} + \frac{log\left(\vartheta_{ki}\right)}{2\sqrt{2Z_3}}\right)\end{aligned} \quad (21)$$

where $Z_3 = \left(h^2_{SU_1} + h^2_{SU_2} + h^2_{SU_3}\right)\gamma_{FC}$. Since $h^2_{SU_1}$, $h^2_{SU_2}$, and $h^2_{SU_3}$ have an exponential distribution, the distribution of their summation Z_3 is given by [33].

$$f_z(Z_3) = \frac{1}{2\gamma^3_{FC}} Z_3^2 \, e^{-Z_3/\gamma_{FC}}, \tag{22}$$

and averaging (21) over (22) yields (24), as shown at the bottom of the next page; the derivation is given in Appendix VII.

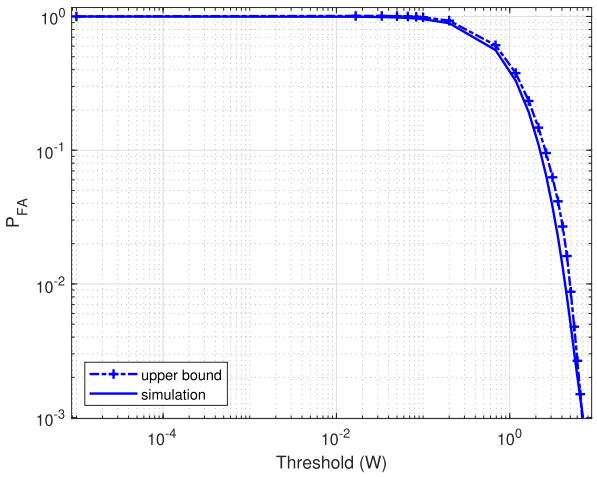

FIGURE 2. Comparison between the simulation results and the upper bound of the false alarm probability for the proposed MAP technique, when SUs' average SNR is 15dB.

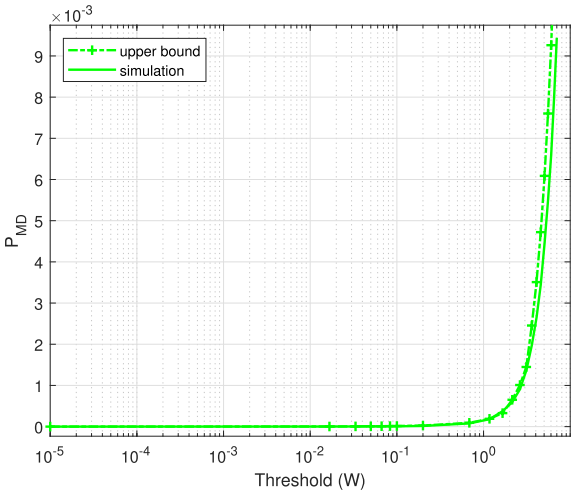

FIGURE 3. Comparison between the simulation results and the upper bound of the misdetection probability for the proposed MAP technique, when SUs' average SNR is 15dB.

TABLE 3. Simulation parameters.

Parameter	Value
Number of SUs (M)	3
Number of PUs	1
SNR at SU receiver (dB)	{13,15,17}
SNR at the FC (dB)	{20,20,20}
Modulation Technique	BPSK
Range of TH used in plotting ROC	$(10^{-4} - 6)$ watt
Channel type	Rayleigh Fading + AWGN
Number of bits/ channel coef. l_h	4
Number of bits/ signal value l_s	6

VI. PERFORMANCE EVALUATION

In this section, the performance of the proposed MAP-based cooperative spectrum sensing technique is evaluated. We started by studying the effect of the detection threshold value at the SUs on the performance of the proposed technique compared to the traditional techniques. Then, we characterize the performance of the system in terms of its probabilities (P_{FA} and P_{MD}) over the feasible Range of Operation (RO) [35]. Then we study the effect of different links quality in terms of different SNR values on the system performance. Finally, the effect of the number of reporting SUs is investigated. The network model used in the evaluation process is depicted in Fig. 1. The default simulation parameters are listed in Table 3 unless otherwise clearly mentioned. All experiments were carried out using MATLAB. The upper bounds for P_{FA} and P_{MD} are shown in Fig. 2 and Fig. 3, respectively. The figures show how much the proposed technique performance is very close to its mathematical upper bounds.

A. THE PROPOSED SYSTEM DETECTION CAPABILITY

In this experiment, we study the PU detection ability of the proposed technique. Fig. 4 shows the value of the FC detection probability P_D against the detection threshold TH. As can be inferred from the figure, the MAP-based technique outperforms other techniques, especially at higher threshold values. Fig. 5 shows the Receiver Operating Characteristic (ROC) of the proposed technique compared to the other combining techniques and its theoretical upper bounds. As can be noticed, the performance of the proposed technique is better than the other combining techniques especially at lower P_{FA} where there are enhancements

$$\begin{aligned} P(CW_k \to CW_i) &= P\left(\|Y_k - HX_i\|^2 - N_0 \, log\left(P(CW_i)\right) < \|Y_k - HX_k\|^2 - N_0 \, log\left(P(CW_k)\right)\right) \\ &= P\left(\|H(X_k - X_i) + \boldsymbol{W}\|^2 + N_0 \, log\left(\frac{P(CW_k)}{P(CW_i)}\right) < \|\boldsymbol{W}\|^2\right) \\ &= P\left(\langle \boldsymbol{W}, \boldsymbol{H}(X_k - X_i)\rangle > \frac{\|H(X_k - X_i)\|^2}{2} + \frac{N_0}{2} \, log\left(\frac{P(CW_k)}{P(CW_i)}\right)\right) \end{aligned} \tag{13}$$

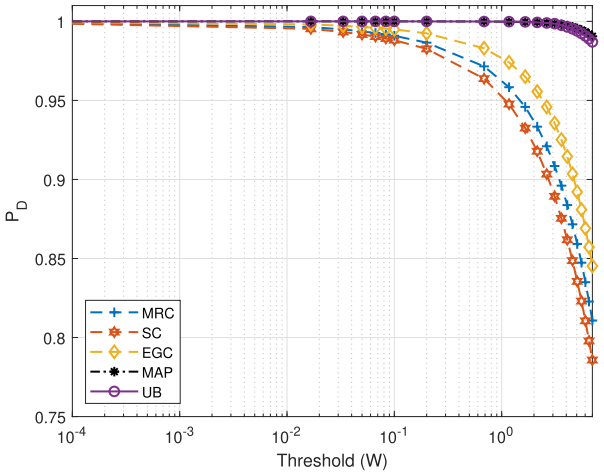

FIGURE 4. Comparison among the proposed MAP, EGC, SC, and MRC using P_D versus threshold in W, when SUs' average SNR is 15dB.

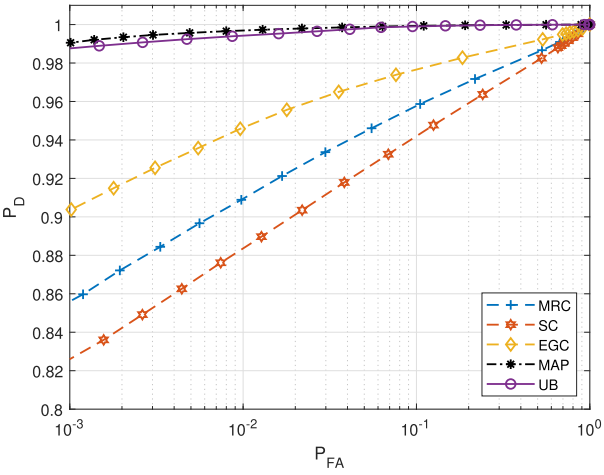

FIGURE 5. System ROC (P_D against P_{FA}) for MRC, SC, EGC, and MAP, when $SNR_1 = 13$dB, $SNR_2 = 15$dB, and $SNR_3 = 17$dB; including the UB curve form the analysis.

in the P_D of about 10%. This means that the proposed system is able to achieve a higher probability of detection at low false alarm probability values compared to the other techniques. To complete the performance analysis, we compare the proposed MAP-Based technique with the progressive MAP proposed in [27]. As can be inferred from Fig. 6, the proposed technique outperforms both the progressive MAP-OR and the progressive MAP-majority techniques especially at low (acceptable) values of P_{FA}.

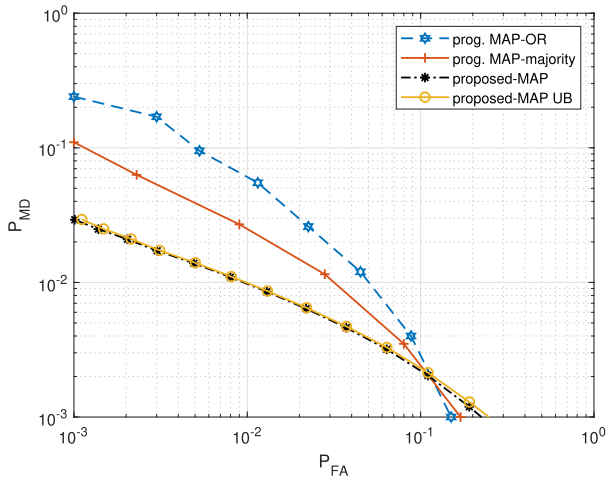

FIGURE 6. A comparison among the proposed MAP, the progressive MAP-OR and the progressive MAP-majority techniques for three SUs and average SNR = 10dB.

The relationship between P_{MD} and P_{FA} can illustrate the overall system performance, which characterizes the ability of the system to make a trade-off between the high ability to detect the presence of the PU and the possibility of triggering a false alarm. The RO, as defined by [35], is a certain region where both P_{MD} and P_{FA} are suitable to be used with general cognitive radio systems, this region extends from 10^{-3} to 10^{-1} for both probabilities. A comparison between the proposed MAP and the other combining techniques, at different values of SNR at the SUs side, is shown in Fig. 7. The comparison shows that the proposed technique outperforms the other techniques, even that for low SNRs where the other combining techniques failed to achieve acceptable results as shown in Fig. 7.b.

$$\rho_2(\vartheta_{ki}) = \begin{cases} \frac{1}{2}\,\vartheta_{ki}^{-\left(1+\frac{1}{\Gamma}\right)/2}\left(1-\Gamma-\frac{\Gamma}{2\,(1+\gamma_{FC})}+\frac{1-\Gamma}{4\Gamma\,(1+\gamma_{FC})}\,log\,\vartheta_{ki}\right), & \text{if} \quad \vartheta_{ki}\geq 1 \\ 1-\frac{1}{2}\,\vartheta_{ki}^{-\left(1-\frac{1}{\Gamma}\right)/2}\left(1+\Gamma+\frac{\Gamma}{2\,(1+\gamma_{FC})}-\frac{1+\Gamma}{4\Gamma\,(1+\gamma_{FC})}\,log\,\vartheta_{ki}\right), & \text{if} \quad \vartheta_{ki}<1. \end{cases} \tag{23}$$

$$\rho_3(\vartheta_{ki}) = \begin{cases} \frac{1}{2}\,\vartheta_{ki}^{-\left(1+\frac{1}{\Gamma}\right)/2}\left(1-\Gamma-\frac{\Gamma}{2\,(1+\gamma_{FC})}+\frac{1-\Gamma}{4\Gamma\,(1+\gamma_{FC})}\,log\,\vartheta_{ki}-\frac{3\Gamma}{8\,(1+\gamma_{FC})^2}\right. \\ \left.+\frac{1-3\Gamma}{16\Gamma\,(1+\gamma_{FC})^2}\,log\,\vartheta_{ki}+\frac{1-\Gamma}{32\Gamma^2\,(1+\gamma_{FC})^2}\,log^2\,\vartheta_{ki}\right), & \text{if} \quad \vartheta_{ki}\geq 1 \\ 1-\frac{1}{2}\,\vartheta_{ki}^{-\left(1-\frac{1}{\Gamma}\right)/2}\left(1+\Gamma+\frac{\Gamma}{2\,(1+\gamma_{FC})}-\frac{1+\Gamma}{4\Gamma\,(1+\gamma_{FC})}\,log\,\vartheta_{ki}+\frac{3\Gamma}{8\,(1+\gamma_{FC})^2}\right. \\ \left.-\frac{1+3\Gamma}{16\Gamma\,(1+\gamma_{FC})^2}\,log\,\vartheta_{ki}+\frac{1+\Gamma}{32\Gamma^2\,(1+\gamma_{FC})^2}\,log^2\,\vartheta_{ki}\right), & \text{if} \quad \vartheta_{ki}<1. \end{cases} \tag{24}$$

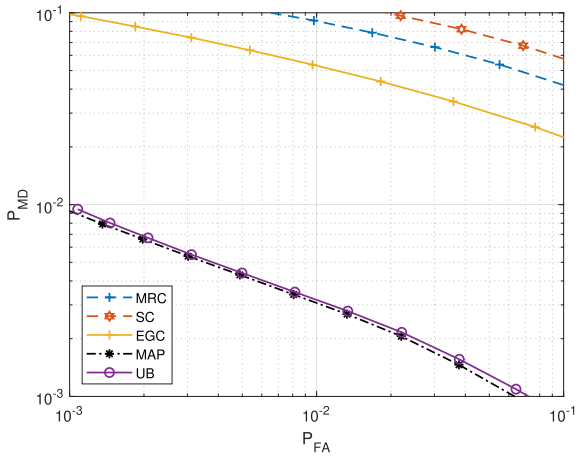

(a) SNR_1=13dB, SNR_2=15dB, and SNR_3=17dB.

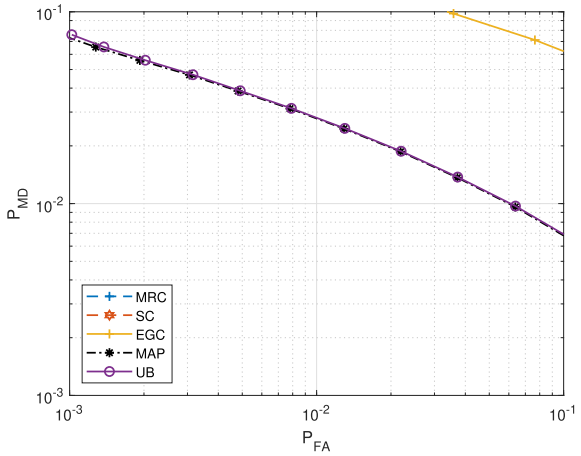

(b) SNR_1=9dB, SNR_2=11dB, and SNR_3=13dB (MRC and SC are not included in the graph as they cannot achieve the performance probabilities defined by our RO for the selected values of SNRs).

FIGURE 7. P_{MD} Vs. P_{FA} for the proposed technique and the other techniques to show the improvement in the overall system performance using different received SNR at SUs.

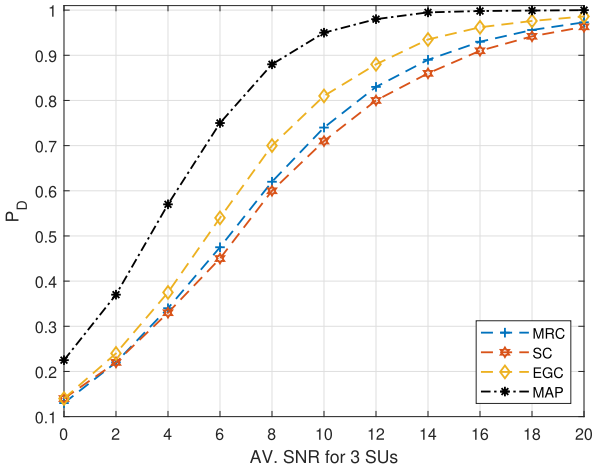

FIGURE 8. System performance (P_D against average SNR) for MRC, SC, EGC, and MAP, when at fixed $P_{FA} = 10^{-2}$.

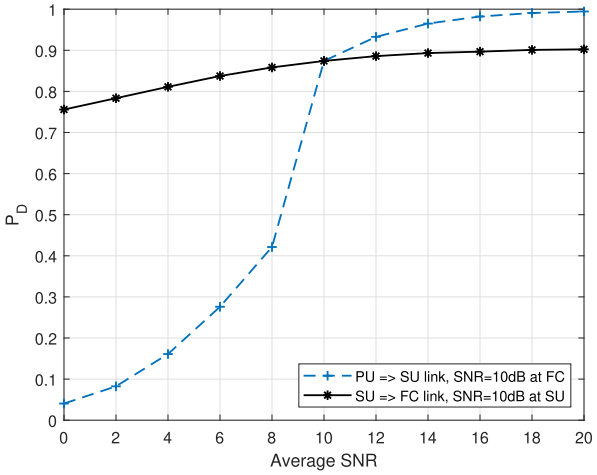

FIGURE 9. The effect of changing the average received SNR at SU and at FC on the system P_D.

The same result can be observed if we compared the system performance in terms of P_D against average SUs' SNR values at a given value of P_{FA} (e.g., $P_{FA} = 10^{-2}$). As shown in Fig. 8, the proposed technique has a much better performance compared to other combining techniques even at lower SNR values. For example, the MAP-based system achieved $P_D = 90\%$ at SNR value = 9dB. However, in order to achieve the same value of P_D with other techniques, the SNR has to reach 13 dB. Also, the P_D value of other combining techniques doesn't exceed 96% when the SNR equals 20 dB; While the proposed MAP-based technique can achieve it at 12 dB SNR.

B. THE EFFECT OF LINKS QUALITY

In this experiment, we investigate the effect of the detection link (PU→ SU) and the reporting link (SU → FC) quality on the system performance. The link quality is expressed by the value of the SNR at the receiving node. Fig. 9 shows the effect of the detection link and the reporting link on the value of P_D. Two curves are plotted, the first one (dashed line) shows the effect of the detection link quality represented by the received SNR at the SU when the SNR at the FC (representing the SU → FC link status) is kept constant at 10dB. In the same way, the second curve (solid line) shows the effect of the reporting link between the SU and the FC at constant SU's SNR. By comparing the two curves, we can conclude that the detection link has a much higher effect on the overall detection process compared to the reporting one.

The full study of the effect of the two links and their combined effect on P_D can be obtained from Fig. 10 which shows the performance of the system at different links status. It generalizes the previous finding that the detection link has a higher effect on the system performance compared to the reporting link.

C. THE EFFECT OF NUMBER OF REPORTING SUs

In this experiment, we investigate the effect of the status and the number of reporting SUs on the detection performance of the system. In the first experiment, we examine the effect

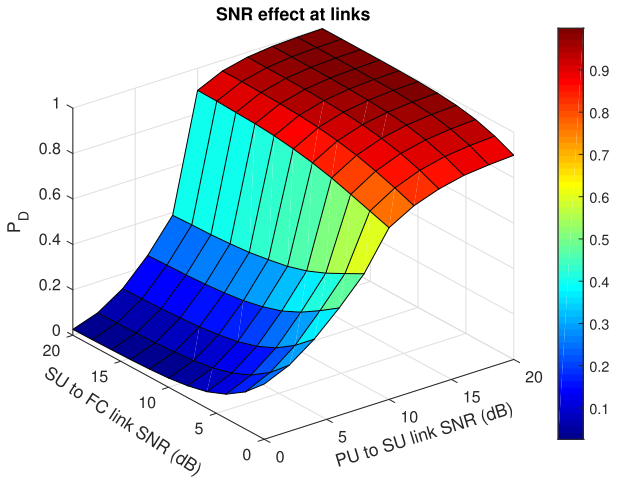

FIGURE 10. The combined effect of the two links quality on the overall system P_D.

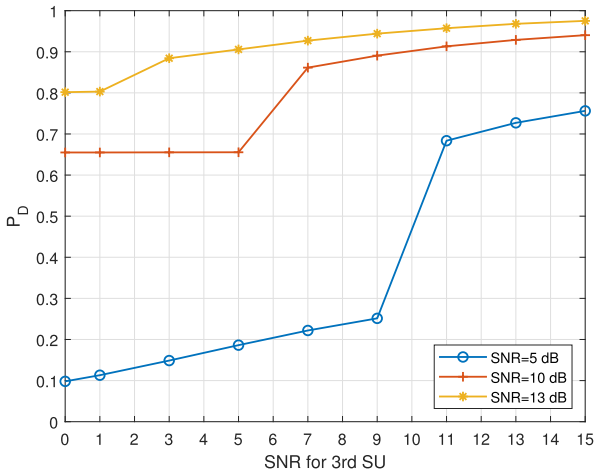

FIGURE 11. The effect of the third SU SNR's on the P_D when the average SNR of the first and second SU is fixed to 5dB, 10dB and 13dB.

of adding an additional SU to the cooperative set of SUs on the overall performance. We assume a set of two SUs with an average SNR value, for which the system achieves a certain probability of detection P_{D_2}. Fig. 11 shows the enchantment in the system performance, in terms of the value of P_D, due to the contribution of the third SU at different average SNR values for the original two SUs. As can be inferred from the figure, there is a threshold value for the third SU's SNR value after which the contribution of third SU becomes noticeably effective in the detection process and enhances the overall system performance. Also, this threshold value has an inversely proportional relation with the average SNR of the original SUs. From this result, it can be inferred that adding a new SU to the cooperative set may not be always useful taking into consideration the additional communication overhead and the increase in detection algorithm computational complexity as will be discussed later.

In the second experiment, we evaluate the effect of the number of reporting SUs on the achieved value of P_D by comparing the performance of the proposed MAP-based technique with that of the other combining techniques for the same number of reporting SUs. As shown in Fig. 12 the MAP-based technique outperforms the other techniques at the same number of SUs especially at low values of average SNR at the SUs.

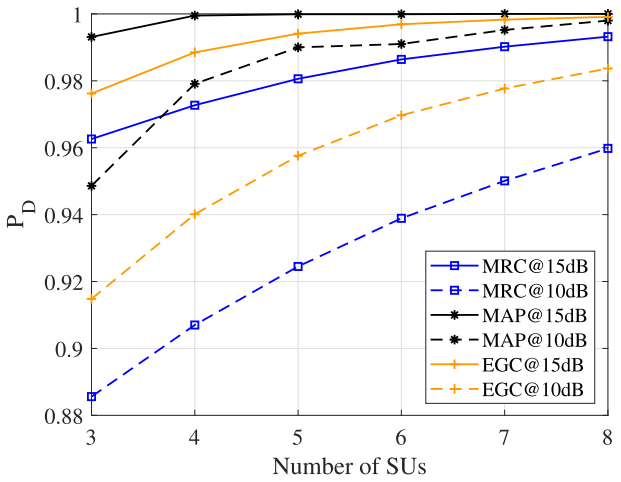

FIGURE 12. The effect of the number of SUs on P_D for average SNR at SU = 10dB, and 15dB and at FC = 20dB.

D. SYSTEM COMPLEXITY

In this section, we calculate the system complexity (O) as a function of the number of reporting SUs for the proposed system as well as the traditional combining techniques. Also, we compare the performance of the proposed techniques (value of P_D) with other traditional techniques. To explain how to get the order of complexity, we need first to calculate the complexity of basic mathematical operations; If we have two numbers of n_1 and n_2 bits, so the complexity order of their addition operation is $O\left(max(n_1, n_2)\right)$, their multiplication operation is $O\left(n_1\, n_2\right)$, and for taking the log operation of n-bit number is $O\left(n^2\, ln\left(n\right)\right)$ [36].

For the proposed algorithm, let l_h, l_s, and l_p be the number of bits representing the channel coefficient h, transmitted signal X from the SU, and the $P(CW_i)$ respectively, and M is the number of SUs. The computational complexity of the proposed MAP technique can be calculated by analyzing the terms of (10) as follows:

- $\|Y - HX_i\|^2$: Since X_i is the BPSK modulated signal corresponding to the i^{th} SU decision bit and only be either $\{+1, -1\}$, the complexity order of this term is $O\left(2M\ (l_s l_h)^2\right)$.
- $log\left(P\left(CW_i\right)\right)$: The complexity order of this term will be $O\left(2^M\ l_p^2\ ln(l_p)\ \right)$.

As the two parts are summed, the complexity order of (10) can be shown as,

$$O\left(2\ max\left(M\ (l_s l_h)^2\ ,\ 2^M\ l_p^2\ ln(l_p)\right)\right)$$

Using the same method for the traditional combining techniques, as defined in [17] and [18], the computational complexity order can be calculated as follows:

- EGC

$$O\left(M\ l_s\ l_h^3\ ln(l_h)\right)$$

- MRC

$$O\left(M\ l_s\ l_h^3\right)$$

- SC

$$O\left(M\ (l_s\ l_h)^2\right)$$

While the previous set of computational complexities show that the MAP-based technique has a higher complexity, it is more fair to compare the complexity for the same performance level. In our case, we should compare the complexity of different systems that achieve the same value of P_D. Assuming that $l_h = 4$, $l_s = 6$, the average SNR value of SUs = 10dB, and the SNR value at the FC = 20dB will be used during the comparison. Fig. 13 shows a comparison between the achieved value of P_D for MAP, EGC, and MRC techniques at nearly the same complexity values.[1] The MAP technique achieves a higher value for P_D for the same complexity.[2] Moreover, for the same complexity value, the MAP-based technique utilizes a smaller set of reporting SUs which means less communication overhead. From the previous analysis, we can notice that the MAP-based technique provides a fair trade-off between the complexity and the performance.

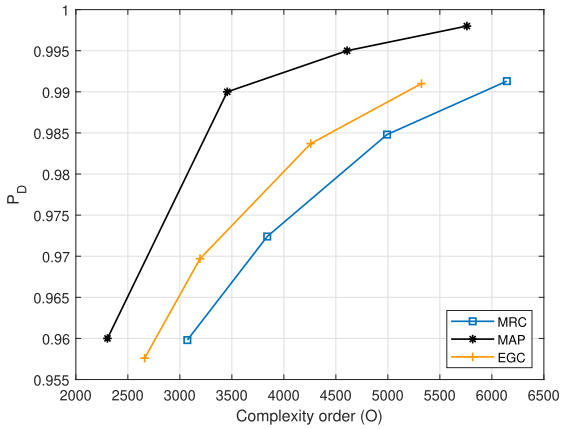

FIGURE 13. The P_D VS. the order of system complexity for the proposed system with average SNR at SUs = 10dB and at FC = 20dB.

VII. CONCLUSION

In this paper, we presented a Maximum A Posteriori (MAP) based cooperative spectrum sensing technique for dynamic spectrum access networks. The proposed technique was implemented at the central fusion center where the individual sensing decisions, regarding the presence of the primary user, are transmitted from the secondary users. The fusion center applies the MAP technique using the collected results to obtain a final estimation regarding the presence of the primary user and disseminated it to the secondary users. Besides the algorithm design, the mathematical upper bounds in terms of the probability of detection and probability of false alarm have been derived for the sake of comparison. The performance of the proposed technique has been compared to that of other techniques found in literature. The results show that our proposed technique outperforms the others in terms of the ability to detect the presence of the primary user represented by enhancing the probability of detection (10% improvement) for the same false alarm probability. Also, the proposed system achieves a better performance in terms of the required number reporting secondary users compared to other techniques for the same probability of detection which compensates for the higher complexity of the system. Also, MAP is considered as a green communication technique by having less power consumption by reducing the number of reporting SUs.

APPENDIXES

APPENDIX A

DERIVATION OF $\rho_1(\vartheta_{ki})$

Averaging (17) over $h^2_{SU_1}$ distribution, and with assumbtion that all channels are Rayleigh flat fading channels with AWGN,

$$\rho_1(\vartheta_{ki}) = \int_0^\infty Q\left(\sqrt{2Z_1} + \frac{log(\vartheta_{ki})}{2\sqrt{2Z_1}}\right) f_Z(Z_1)\, dz \quad (25)$$

where $Z_1 = h^2_{SU_1}\gamma_{FC}$, and

$$f_Z(Z_1) = \frac{1}{\gamma_{FC}}\, e^{\left(\frac{-Z_1}{\gamma_{FC}}\right)}$$

Substituting $f_Z(Z_1)$ into (25) taking in consideration that $Q(\nu) = 0.5\ \text{erfc}\left(\frac{\nu}{\sqrt{2}}\right)$

$$\rho_1(\vartheta_{ki}) = \frac{1}{2\gamma_{FC}} \int_0^\infty \text{erfc}\left(\sqrt{Z_1} + \frac{C}{\sqrt{Z_1}}\right) e^{\left(\frac{-Z_1}{\gamma_{FC}}\right)} dz \quad (26)$$

where $C = \frac{log(\vartheta_{ki})}{4}$. Integrating (26) using integration by parts where $U = \text{erfc}\left(\sqrt{Z_1} + \frac{C}{\sqrt{Z_1}}\right)$, $dV = e^{\left(\frac{-Z_1}{\gamma_{FC}}\right)} dz$, $dU = \frac{-1}{\sqrt{\pi Z_1}}\left(1 - \frac{C}{Z_1}\right) e^{\frac{-(Z_1+C)^2}{Z_1}} dx$, and $V = -\gamma_{FC} e^{\left(\frac{-Z_1}{\gamma_{FC}}\right)}$ yields

$$\rho_1(\vartheta_{ki}) = \frac{1}{2\gamma_{FC}} \left[\gamma_{FC}\ \text{erfc}\left(\sqrt{Z_1} + \frac{C}{\sqrt{Z_1}}\right) e^{\left(\frac{-Z_1}{\gamma_{FC}}\right)} - \frac{\gamma_{FC}}{\sqrt{\pi}} \int \frac{1}{\sqrt{Z_1}}\left(1 - \frac{C}{Z_1}\right) e^{-\frac{Z_1}{\gamma_{FC}} - \frac{(Z_1+C)^2}{Z_1}} dz \right]_0^\infty \quad (27)$$

$$= \begin{cases} T_1 & C \geq 0 \\ 1 + T_1 & C < 0 \end{cases} \quad (28)$$

where

$$T_1 = -\frac{1}{2\sqrt{\pi}} \int_0^\infty \frac{1}{\sqrt{Z_1}}\left(1 - \frac{C}{Z_1}\right) e^{-\frac{Z_1}{\gamma_{FC}} - \frac{(Z_1+C)^2}{Z_1}} dz \quad (29)$$

[1] SC technique is excluded from this comparison as its P_D will be equal to the highest P_D received from SUs

[2] Here, we change the complexity by changing the number of reporting SUs and fixing the other parameters like l_h and l_s.

after some manipulations, (29) can written as

$$T_1 = -\frac{e^{-r}}{2\sqrt{\pi}} \int_0^{\infty} \frac{1}{\sqrt{u}} \left(\Gamma - \frac{d}{u}\right) e^{-\frac{(u+d)^2}{u}} du \tag{30}$$

where $r = 2b\left(1 - \sqrt{1 + \frac{1}{\gamma_{FC}}}\right)$, $d = C\sqrt{1 + \frac{1}{\gamma_{FC}}}$, and $u = Z_1\left(1 + \frac{1}{\gamma_{FC}}\right)$. (30) can be written as follows

$$\begin{aligned} T_1 &= -\frac{e^{-r}}{2\sqrt{\pi}} \int_0^{\infty} \frac{1}{\sqrt{u}} \left(-1 + \Gamma + 1 - \frac{d}{u}\right) e^{-\frac{(u+d)^2}{u}} du \\ &= (1-\Gamma)\frac{e^{-r}}{2\sqrt{\pi}} \int_0^{\infty} \frac{1}{\sqrt{u}} e^{-\frac{(u+d)^2}{u}} du \\ &\quad - \frac{e^{-r}}{2\sqrt{\pi}} \left[\operatorname{erfc}\left(\sqrt{u} + \frac{d}{\sqrt{u}}\right)\right]_0^{\infty} \qquad (31) \\ &= \begin{cases} T_1^* & C \geq 0 \\ 1 + T_1^* & C < 0 \end{cases} \qquad (32) \end{aligned}$$

where

$$T_1^* = (1-\Gamma)\frac{e^{-r}}{2\sqrt{\pi}} \int_0^{\infty} \frac{1}{\sqrt{u}} e^{-\frac{(u+d)^2}{u}} du \tag{33}$$

By changing variables, let $y = \sqrt{u}$, $dy = \frac{du}{2\sqrt{u}}$, and after substitution in (33)

$$\begin{aligned} T_1^* &= (1-\Gamma)\frac{e^{-r}}{\sqrt{\pi}} \int_0^{\infty} e^{-\left(\frac{y^2+d}{y}\right)^2} dy \\ &= (1-\Gamma)\frac{e^{-(2d+r)}}{\sqrt{\pi}} \int_0^{\infty} e^{-y^2 - \frac{d^2}{y^2}} dy \qquad (34) \end{aligned}$$

Using Mathematica to find the integral in (34) yields

$$T_1^* = \begin{cases} \frac{1}{2}(1-\Gamma)\, e^{-4d-r} & C \geq 0 \\ \frac{1}{2}(1+\Gamma)\, e^{-r} & C < 0 \end{cases} \tag{35}$$

After substituting for the d, r and C,

$$T_1^* = \begin{cases} \frac{1}{2}(1-\Gamma)\, \vartheta_{ki}^{-\frac{1}{2}(1+1/\Gamma)} & \vartheta_{ki} \geq 1 \\ \frac{1}{2}(1+\Gamma)\, \vartheta_{ki}^{-\frac{1}{2}(1-1/\Gamma)} & \vartheta_{ki} < 1 \end{cases} \tag{36}$$

Substituting from (36) into (32) then into (28) yields (18)

APPENDIX B
DERIVATION OF $\rho_2(\vartheta_{ki})$

Consider the case when $k = 4$ and $i = 6$ (which have two different bits belong to SU_1,and SU_3), and averaging (19) over the distribution of Z_2 (20) yields

$$\rho_2(\vartheta_{46}) = \frac{1}{2\gamma_{FC}^2} \int_0^{\infty} \operatorname{erfc}\left(\sqrt{Z_2} + \frac{C}{\sqrt{Z_2}}\right) Z_2\, e^{-\frac{Z_2}{\gamma_{FC}}} dz \tag{37}$$

where $C = \frac{log(\vartheta_{ki})}{4}$. Integrating (37) using integration by parts where: $dV = Z_2\, e^{-\frac{Z_2}{\gamma_{FC}}} dz$, $U = \operatorname{erfc}\left(\sqrt{Z_2} + \frac{C}{\sqrt{Z_2}}\right)$, $dU = \frac{-1}{\sqrt{\pi Z_2}}\left(1 - \frac{C}{Z_2}\right) e^{\frac{-(Z_2+C)^2}{Z_2}} dZ$, and $V = \left[-\gamma_{FC}(\gamma_{FC} + Z_2)\, e^{-Z_2/\gamma_{FC}}\right]_0^{\infty}$ yields

$$\begin{aligned} &\rho_2(\vartheta_{ki}) \\ &= \frac{1}{2\gamma_{FC}^2} \\ &\quad \left[-\gamma_{FC}(\gamma_{FC} + Z_2)\, e^{-Z_2/\gamma_{FC}} \operatorname{erfc}\left(\sqrt{Z_2} + \frac{C}{\sqrt{Z_2}}\right)\right. \\ &\quad \left. - \frac{\gamma_{FC}}{\sqrt{\pi}} \int \frac{1}{\sqrt{Z_2}} (\gamma_{FC} + Z_2)\left(1 - \frac{C}{Z_2}\right) e^{\frac{-(Z_2+C)^2}{Z_2} - \frac{Z_2}{\gamma_{FC}}} dz\right]_0^{\infty} \\ &= \begin{cases} T_2 & C \geq 0 \\ 1 - T_2 & C < 0 \end{cases} \qquad (38) \end{aligned}$$

where

$$\begin{aligned} T_2 &= \frac{1}{2\gamma_{FC}\sqrt{\pi}} \\ &\quad \times \int_0^{\infty} \frac{1}{\sqrt{Z_2}} (\gamma_{FC} + Z_2)\left(1 - \frac{C}{Z_2}\right) e^{\frac{-(Z_2+C)^2}{Z_2} - \frac{Z_2}{\gamma_{FC}}} dz. \end{aligned} \tag{39}$$

Using Mathematica to solve this integration yields

$$\begin{aligned} &T_2 \\ &= \begin{cases} \frac{1}{2}\left(1 - \Gamma - \frac{1}{1+\gamma_{FC}}\left(\Gamma\left(\frac{1}{2} + d\right) - d\right)\right) e^{-4d-r} & C \geq 0 \\ \frac{1}{2}\left(1 + \Gamma - \frac{1}{1+\gamma_{FC}}\left(\Gamma\left(\frac{1}{2} - d\right) - d\right)\right) e^{-r} & C < 0. \end{cases} \end{aligned} \tag{40}$$

Substituting back for r,d,and C then using (40) in (38), and after some mathematical manipulations, (23) is obtained.

APPENDIX C
DERIVATION OF $\rho_3(\vartheta_{ki})$

Consider the case when $k = 2$ and $i = 7$ (which have three different bits belong to SU_1, SU_2, and SU_3). Averaging (21) over the distribution of Z_3 (22) yields

$$\rho_3(\vartheta_{27}) = \frac{1}{4\gamma_{FC}^3} \int_0^{\infty} \operatorname{erfc}\left(\sqrt{Z_3} + \frac{C}{\sqrt{Z_3}}\right) Z_3^2\, e^{-\frac{Z_3}{\gamma_{FC}}} dz \tag{41}$$

where $C = \frac{log(\vartheta_{ki})}{4}$. Integrating (41) using integration by parts where: $dV = Z_3^2\, e^{-\frac{Z_3}{\gamma_{FC}}} dz$, $U = \operatorname{erfc}\left(\sqrt{Z_3} + \frac{C}{\sqrt{Z_3}}\right)$, $dU = \frac{-1}{\sqrt{\pi Z_3}}\left(1 - \frac{C}{Z_3}\right) e^{\frac{-(Z_3+C)^2}{Z_3}} dZ$, and $V = \left[(-\gamma_{FC}Z_3^2 - 2\gamma_{FC}^2 - 2\gamma_{FC}Z_3)\, e^{-Z_3/\gamma_{FC}}\right]_0^{\infty}$ yields

$$\begin{aligned} &\rho_3(\vartheta_{ki}) \\ &= \frac{1}{4\gamma_{FC}^3} \left[\operatorname{erfc}\left(\sqrt{Z_3} + \frac{C}{\sqrt{Z_3}}\right) e^{-Z_3/\gamma_{FC}} (-\gamma_{FC}Z_3^2\right. \\ &\quad \left. - 2\gamma_{FC}^2 - 2\gamma_{FC}Z_3) - \frac{\gamma_{FC}}{\sqrt{\pi}} \int \frac{-Z_3^2 - 2\gamma_{FC} - 2Z_3}{\sqrt{Z_3}} (1\right. \\ &\quad \left. - \frac{C}{Z_3}) e^{\frac{-(Z_3+C)^2}{Z_3} - \frac{Z_3}{\gamma_{FC}}} dz\right]_0^{\infty} \end{aligned} \tag{42}$$

$$= \begin{cases} T_3 & C \geq 0 \\ 1 - T_3 & C < 0 \end{cases} \quad (43)$$

where

$$T_3 = \frac{1}{4\gamma_{FC}^2\sqrt{\pi}} \int \frac{-Z_3^2 - 2\gamma_{FC} - 2Z_3}{\sqrt{Z_3}} \left(1 - \frac{C}{Z_3}\right) e^{\frac{-(Z_3+C)^2}{Z_3} - \frac{Z_3}{\gamma_{FC}}} dz. \quad (44)$$

Using Mathematica to solve this integration and substituting back in (43), and after some mathematical manipulations, (24) is obtained.

REFERENCES

[1] S. D. A. Nkalango, H. Zhao, Y. Song, and T. Zhang, "Energy efficiency under double deck relay assistance on cluster cooperative spectrum sensing in hybrid spectrum sharing," *IEEE Access*, vol. 8, pp. 41298–41308, 2020.

[2] M. McHenry, *NSF Spectrum Occupancy Measurements Project Summary*. Vienna, VA, USA: Shared Spectrum Company, 2005.

[3] C. Sun and R. Jiao, "Discrete exclusion zone for dynamic spectrum access wireless networks," *IEEE Access*, vol. 8, pp. 49551–49561, 2020.

[4] W. Liang, S. X. Ng, and L. Hanzo, "Cooperative overlay spectrum access in cognitive radio networks," *IEEE Commun. Surveys Tuts.*, vol. 19, no. 3, pp. 1924–1944, 3rd Quart., 2017.

[5] F. Awan, N. Sheikh, and M. Hanif, *Information Theory of Cognitive Radio System*. London, U.K.: IntechOpen, Nov. 2009.

[6] J. Pastircak, J. Gazda, and D. Kocur, "A survey on the spectrum trading in dynamic spectrum access networks," in *Proc. ELMAR*, Sep. 2014, pp. 1–4.

[7] W. S. H. M. W. Ahmad, N. A. M. Radzi, F. S. Samidi, A. Ismail, F. Abdullah, M. Z. Jamaludin, and M. N. Zakaria, "5G technology: Towards dynamic spectrum sharing using cognitive radio networks," *IEEE Access*, vol. 8, pp. 14460–14488, 2020.

[8] Ridhima and A. Singh Buttar, "Fundamental operations of cognitive radio: A survey," in *Proc. IEEE Int. Conf. Electr., Comput. Commun. Technol. (ICECCT)*, Feb. 2019, pp. 1–5.

[9] I. Gupta, A. Hari, and O. P. Sahu, "Hardware implementation of energy detection scheme in cognitive radio networks," in *Proc. Int. Conf. Comput., Power Commun. Technol. (GUCON)*, Sep. 2018, pp. 575–577.

[10] S. MacDonald, D. C. Popescu, and O. Popescu, "Analyzing the performance of spectrum sensing in cognitive radio systems with dynamic PU activity," *IEEE Commun. Lett.*, vol. 21, no. 9, pp. 2037–2040, Sep. 2017.

[11] G. I. Tsiropoulos, O. A. Dobre, M. H. Ahmed, and K. E. Baddour, "Radio resource allocation techniques for efficient spectrum access in cognitive radio networks," *IEEE Commun. Surveys Tuts.*, vol. 18, no. 1, pp. 824–847, 1st Quart., 2016.

[12] M. Karimi, S. M. S. Sadough, and M. Torabi, "Optimal cognitive radio spectrum access with joint spectrum sensing and power allocation," *IEEE Wireless Commun. Lett.*, vol. 9, no. 1, pp. 8–11, Jan. 2020.

[13] N. H. Kamil and X. Yuan, "Detection proposal schemes for spectrum sensing in cognitive radio," *Wireless Sensor Netw.*, vol. 2, no. 5, pp. 365–372, 2010.

[14] V. Ramani and S. K. Sharma, "Cognitive radios: A survey on spectrum sensing, security and spectrum handoff," *China Commun.*, vol. 14, no. 11, pp. 185–208, Nov. 2017.

[15] I. F. Akyildiz, B. F. Lo, and R. Balakrishnan, "Cooperative spectrum sensing in cognitive radio networks: A survey," *Phys. Commun.*, vol. 4, no. 1, pp. 40–62, Mar. 2011.

[16] A. Sharmila and P. Dananjayan, "Spectrum sharing techniques in cognitive radio networks—A survey," in *Proc. IEEE Int. Conf. Syst., Comput., Autom. Netw. (ICSCAN)*, Mar. 2019, pp. 1–4.

[17] N. Kaur, "SNR and BER performance analysis of MRC and EGC receivers over Rayleigh fading channel," *Int. J. Comput. Appl.*, vol. 132, no. 9, pp. 12–17, Dec. 2015.

[18] M. S. Danijela Aleksic and D. Krstic, "Outage probability comparison of mrc, egc and sc receivers over short term fading channels," *Int. J. Commun.*, vol. 1, pp. 104–109, 2016.

[19] S.-C. Lin and Y.-C. Chiang, "Performance analysis for optimum transmission and comparison with maximal ratio transmission for MIMO systems with cochannel interference," in *Proc. 8th Int. Conf. Inf., Commun. Signal Process.*, Dec. 2011, pp. 1–5.

[20] A. Rauniyar, J. M. Jang, and S. Y. Shin, "Optimal hard decision fusion rule for centralized and decentralized cooperative spectrum sensing in cognitive radio networks," *J. Adv. Comput. Netw.*, vol. 3, no. 3, pp. 207–212, 2015.

[21] D. Hamza, S. Aissa, and G. Aniba, "Equal gain combining for cooperative spectrum sensing in cognitive radio networks," *IEEE Trans. Wireless Commun.*, vol. 13, no. 8, pp. 4334–4345, Aug. 2014.

[22] R. Sharma and J. Wallace, "Analysis of fusion and combining for wireless source detection," in *Proc. Int. ITG Workshop Smart Antennas*, Feb. 2009, pp. 16–18.

[23] S. Nallagonda, S. Dhar Roy, S. Kundu, G. Ferrari, and R. Raheli, "Performance of MRC fusion-based cooperative spectrum sensing with censoring of cognitive radios in Rayleigh fading channels," in *Proc. 9th Int. Wireless Commun. Mobile Comput. Conf. (IWCMC)*, Jul. 2013, pp. 30–35.

[24] J. Luo and X. He, "A soft-hard combination decision fusion scheme for a clustered distributed detection system with multiple sensors," *Sensors*, vol. 18, no. 12, pp. 1–18, Dec. 2018. [Online]. Available: https://www.ncbi.nlm.nih.gov/pmc/articles/PMC6308585/

[25] A. Maleki, D. Mirzahosseini, and N. A. Moghaddam, "Cooperative Bayesian-based detection framework for spectrum sensing in cognitive radio networks," *IET Commun.*, vol. 13, no. 15, pp. 2280–2284, Sep. 2019.

[26] X. Bai, M. Hao, and W. Wang, "Frequency spectrum sensing of cognitive radio based on Bayesian network," in *Proc. 8th Int. Congr. Image Signal Process. (CISP)*, Oct. 2015, pp. 1095–1099.

[27] G. Zhou, J. Wu, and K. Sohraby, "Cooperative spectrum sensing with a progressive MAP detection algorithm," in *Proc. IEEE Global Telecommun. Conf. GLOBECOM*, Dec. 2011, pp. 1–5.

[28] H. Mohammed and T. A. Khalaf, "Optimal positioning of relay node in wireless cooperative communication networks," in *Proc. 9th Int. Comput. Eng. Conf. (ICENCO)*, Dec. 2013, pp. 122–127.

[29] R. Bassett and J. Deride, "Maximum a posteriori estimators as a limit of bayes estimators," *Math. Program.*, vol. 174, nos. 1–2, pp. 129–144, Mar. 2019, doi: 10.1007/s10107-018-1241-0.

[30] M. Tahir, M. Hadi Habaebi, and M. R. Islam, "Novel distributed algorithm for coalition formation for enhanced spectrum sensing in cognitive radio networks," *AEU Int. J. Electron. Commun.*, vol. 77, pp. 139–148, Jul. 2017.

[31] H. J. C. Tellambura and S. Atapattu, *Conventional Energy Detector*. New York, NY, USA Springer, 2014, pp. 11–26.

[32] O. Altrad and S. Muhaidat, "A new mathematical analysis of the probability of detection in cognitive radio over fading channels," *EURASIP J. Wireless Commun. Netw.*, vol. 2013, no. 1, p. 159, Dec. 2013.

[33] A. Goldsmith, *Wireless Communications*. Cambridge, U.K.: Cambridge Univ. Press, 2005.

[34] P. Oguntunde, O. Odetunmibi, and A. O. Adejumo, "On the sum of exponentially distributed random variables: A convolution approach," *Eur. J. Statist. Probab.*, vol. 2, pp. 1–8, 03 2014.

[35] A. Tohamy, U. S. Mohammed, and T. A. Khalaf, "Cooperative sensing using maximum a posteriori as a detection technique in cognitive radio network," in *Proc. 36th Nat. Radio Sci. Conf. (NRSC)*, Apr. 2019, pp. 266–272.

[36] S. Arora and B. Barak, *Computational Complexity: A Modern Approach*, 1st ed. Cambridge, U.K.: Cambridge Univ. Press, Jun. 2009, p. 594.

AHMED TOHAMY was born in Assiut, Egypt, in 1982. He received the B.Sc and M.Sc degrees in electrical engineering from Assiut University, Assiut, in 2004 and 2014, respectively, where he is currently pursuing the Ph.D. degree. From 2004 to 2016, he was a System Engineer with Assiut University. From 2016 to 2018, he was a Lecturer with the Electrical Department, Faculty of Engineering, Tabuk University, Saudi Arabia.

USAMA SAYED MOHAMED received the B.Sc. and M.Sc. degrees in electrical engineering from Assiut University, Assiut, Egypt, and the Ph.D. degree in electrical engineering from Czech Technical University in Prague, Czech Republic. From November 1999 to February 2000, he was a Research Assistant with the University of California at Santa Barbara (UCSB), USA. From November 2001 to April 2002, he was a Postdoctoral Fellow with the Faculty of Engineering, Czech Technical University in Prague. He was the Head of the Electrical Engineering Department. He was the Vice Dean for Graduate Studies and Research with the Faculty of Engineering, Assiut University. He is currently a Professor with the Faculty of Engineering, Assiut University. He has authored or coauthored more than 150 scientific articles, three undergraduate books, and some chapters in reference books. His research interests include signal processing, wireless communications technology, wireless networks, image coding, statistical signal processing, blind signal separation, and video coding. He was given several awards, including the Soliman Hozain Award of Engineering Science, in 2007, the Best Paper Award in Electrical Engineering from Assiut University, in 2005, and the Best Paper Award in the two conferences NRSC2018 and NRSC2019. He acts as a Reviewer and a member of the editorial board for several scientific journals and conferences. He has been selected for the inclusion in 2010 Edition of the USA-Marquis Who's Who in the World. He is a Reviewer for the Quality Assurance and Accreditation of Egyptian for Higher Education and the Quality Assurance of the special program in the Ministry of Higher Education in Egypt. He is the National Key Facilitator (NKF) from International Labor Organization (ILO) in the entrepreneurship.

MOHAMMAD M. ABDELLATIF (Senior Member, IEEE) received the B.Sc. degree in electronics and communications engineering from Assiut University, Assiut, Egypt, in 2004, the M.Sc. degree in telecommunication engineering from the King Fahd University of Petroleum and Minerals, Dhahran, Saudi Arabia, in 2006, and the Ph.D. degree in telecommunications engineering from the Electrical and Computer Engineering Department, University of Porto, Portugal, in 2015. He is currently a full-time Lecturer with The British University in Egypt. He received a four-year scholarship from the Foundation of science and technology of Portugal (FCT) for his Ph.D, as well as a one year CMU Porto Joint Research Project Award (SELF-PVP). He has been served as a Reviewer for many IEEE conferences, and the IEEE TRANSACTIONS ON COMMUNICATIONS and the IEEE JOURNAL IN SELECTED AREAS IN COMMUNICATION (JSAC).

TAHA A. KHALAF (Member, IEEE) received the B.Sc. and M.Sc. degrees in electrical engineering from Assiut University, Assiut, Egypt, in 2000 and 2004, respectively, and the Ph.D. degree from Iowa State University, Ames, IA, USA, in May 2011. He is currently an Associate Professor with the Department of Electrical Engineering, Assiut University. His major research interests include wireless communications include cooperative communications, network coding, cognitive radio, and physical layer security. He received ECEB Washington DC grant 2006–2010. He received excellence awards during his study from Mobinil, Six October University, and the Egyptian Syndicate of Engineers.

MOHAMED ABDELRAHEEM (Member, IEEE) received the B.Sc. and M.Sc. degrees in electrical engineering from Assiut University, Egypt, in 2004 and 2010, respectively, and the Ph.D. degree in electrical engineering from Virginia Tech, in 2015. He is currently an Assistant Professor of electrical engineering with Assiut University. His research interests include wireless networking, the Internet of Things, and embedded systems design. He has been a PI and Co-PI for a number of research projects from Egyptian funding entities, such as STDF, NTRA, and ITIDA. He is a Royal Academy of Engineering-leaders in Innovations Fellow. He has been serving as a Reviewer for a number of IEEE conferences and journals.